Available online at www.sciencedirect.com
SCIENCE DIRECT®
International Journal of Heat and Mass Transfer 48 (2005) 4657–4666
International Journal of HEAT and MASS TRANSFER
www.elsevier.com/locate/ijhmt

Finite volume method in 3-D curvilinear coordinates with multiblocking procedure for radiative transport problems

P. Talukdar *, M. Steven, F.V. Issendorff, D. Trimis

Institute of Fluid Mechanics (LSTM), University of Erlangen-Nuremberg, Cauerstrasse 4, D 91058 Erlangen, Germany

Received 22 December 2004; received in revised form 4 May 2005

Abstract

The finite volume method of radiation is implemented for complex 3-D problems in order to use it for combined heat transfer problems in connection with CFD codes. The method is applied for a 3-D block structured grid in a radiatively participating medium. The method is implemented in non-orthogonal curvilinear coordinates so that it can handle irregular structure with a body-fitted structured grid. The multiblocking is performed with overlapping blocks to exchange the information between the blocks. Five test problems are considered in this work. In the first problem, present work is validated with the results of the literature. To check the accuracy of multiblocking, a single block is divided into four blocks and results are validated against the results of the single block simulated alone in the second problem. Complicated geometries are considered to show the applicability of the present procedure in the last three problems. Both radiative and non-radiative equilibrium situations are considered along with an absorbing, emitting and scattering medium.

Keywords: Radiation; Participating media; Finite volume method; Multiblocking

1. Introduction

The finite volume method (FVM) is one of the popular methods used in computational fluid dynamics (CFD) and has been extensively used in many of its applications. In radiative heat transfer through participating media, there are quite a lot of methods that have been used by researchers over the past years. Among them, the FVM is also a promising method which use has significantly been increased during the last decade [1–7]. For the problems involving combined conduction, convection and radiation, it is always convenient to use the same grid philosophy which eliminates the need to interpolate variables like temperature, incident radiation etc. The FVM is an alternative for this and has been found to be very promising for the problems with radiation and CFD applications.

The FVM has been applied for many different situations by the researchers. It has been applied for 2-D and 3-D Cartesian and cylindrical geometries, orthogonal and non-orthogonal curvilinear coordinates, 2-D block structured grids and also for 3-D unstructured grids. The method is not yet implemented for 3-D block structured grids and that is the motivation for the present work.

* Corresponding author. Tel.: +49 9131 8529489; fax: +49 9131 8529503.
E-mail address: prabal_iitg@yahoo.com (P. Talukdar).

0017-9310/$ - see front matter © 2005 Elsevier Ltd. All rights reserved.
doi:10.1016/j.ijheatmasstransfer.2005.06.001

Nomenclature

a	coefficient of the discretization equation
A	area of control volume faces
b	source term in the discretization equation
D_c^l	direction cosine integrated over $\Delta\Omega^l$
$\hat{e}$	unit vector
f	weight factor for interpolation
g	non-dimensional incident radiant energy $(=\frac{G}{\sigma T_{ref}^4})$
G	incident radiant energy
I	intensity
m	total number of angular directions
$\hat{n}$	unit outward normal vector
$\hat{r}$	position vector
s	distance traveled by a beam
S	source function
T	temperature
T_h	temperature of the hot boundary
T_{ref}	reference temperature
wf_k	weight factor for incident radiation
wfx_k, wfy_k, wfz_k	weight factor in x-, y- and z-direction for heat flux
x, y, z	coordinate direction

Greek symbols

β	extinction coefficient
ΔV	volume of a control volume
$\Delta\Omega^l$	control angle
ε	emissivity
κ	absorption coefficient
μ, ξ, η	direction cosines in x-, y- and z-directions
θ	polar angle
σ	Stefan–Boltzmann constant or scattering coefficient
ϕ	azimuthal angle
Φ	scattering phase function
ω	scattering albedo $(=\frac{\sigma}{\beta})$

Subscripts

b	blackbody
E, W, N, S, B,T	east, west, north, south, bottom and top neighbors of P
e, w, n, s, b, t	east, west, north, south, bottom and top control-volume faces
h	hot boundary
m	medium
P	control volume point
x, y, z	coordinate directions

Superscript

l'	angular directions

Looking back to the history of the FVM in radiative transfer, Chui and co-workers [1,2] proposed this method around 1990. They implemented this method for Cartesian meshes [1] and also for cylindrical meshes [2]. They also implemented it for non-orthogonal boundary-fitted meshes [3]. A slightly different control volume approach is adopted by Chai and his co-workers [4–7] for the FVM in radiation. Their FVM calculation procedure is compatible with the control volume approaches of Karki and Patankar [8–10], Demirdzic et al. [11], Peric [12], Shyy et al. [13], and Rhie and Chow [14]. The present work is also based on this approach. Chai et al. [4] discussed the FVM for 2-D and 3-D Cartesian enclosures with collimated radiation and heat generation. They used step and exponential scheme for finding out the face intensities and considered an absorbing, emitting and anisotropically scattering media. In other works [5–7], they have implemented FVM for irregular geometries. They used a Cartesian based blocked-off region concept [5] and body-fitted coordinate system [6] to simulate different irregular structures in a 2-D domain. They used multiblock procedure [7] to simulate 2-D complex geometries and discussed the advantages associated with this approach compared to blocked-off region concept and body-fitted meshes. As far as unstructured mesh is concerned, Murthy and Mathur [15] have extended the FVM for radiation for arbitrary geometries with meshes composed of convex polyhedra. They extended the same methodology for axisymmetric geometries [16].

The block-structured grid is a very popular method in CFD because of its accuracy and flexibility to complicated geometries. Although, in the present days, unstructured grids are used mainly in industrial problems due to the complexity of the geometries, but still there are many problems which can be solved by structured grids. The structured grids are more accurate than the unstructured one and have considerably less memory requirement compared to the unstructured meshes for the same level of accuracy. Keeping in mind these advantages, the aim of this work is to generate a code which can be coupled to a similar CFD code for combined heat transfer processes. The FVM for radiation also uses the same methodology as applied to block structured grids in CFD. The information from one block to another is copied with the help of overlapping blocks and thus suffers no errors with the blocking procedure. For a test case, one single block is divided into

four blocks to compare the results of the four blocks with the single block. Since the block transforms the information with overlapping blocks, the method remains conservative also for multiblock. The multiblocking in radiation is previously done by Chai and Moder [7] in a 2-D domain. They did it for straight and curved interphases between the blocks. They also considered matching and non-matching grids between different blocks. They made an energy balance between the blocks to calculate the intensities in the interface. They did not use any overlapping blocks like the present work.

This work is presented with five test problems. First the 3-D code is validated with the available results for a single block. The multiblocking procedure is validated in the second problem. Then other three test problems of irregular structures are considered which are either validated or justified with reasoning.

2. Mathematical formulation

The radiative transfer equation (RTE) for a gray absorbing, emitting and scattering medium in the direction $\hat{s}$ can be written as

$$\frac{\mathrm{d}I(\vec{r},\hat{s})}{\mathrm{d}s} = -\beta(\vec{r})I(\vec{r},\hat{s}) + S(\vec{r},\hat{s}) \tag{1}$$

where the source function can be defined as

$$S(\vec{r},\hat{s}) = \kappa(\vec{r})I_{\mathrm{b}}(\vec{r}) + \frac{\sigma(\vec{r})}{4\pi}\int I(\vec{r},\hat{s}')\Phi(\hat{s}',\hat{s})\,\mathrm{d}\Omega' \tag{2}$$

In Eqs. (1) and (2), $\vec{r}$ and $\hat{s}$ are the position vector and the unit vector describing the radiative intensity direction, respectively.

The discretization procedure of RTE is according to that of Chai et al. [4] and is not repeated here. Integrating the RTE (Eq. (1)) over a 3-D control volume (Fig. 1(a)) and over a control angle (Fig. 1(b)), the final discretized equation can be written as

$$a_{\mathrm{P}}^{l}I_{\mathrm{P}}^{l} = a_{\mathrm{W}}^{l}I_{\mathrm{W}}^{l} + a_{\mathrm{E}}^{l}I_{\mathrm{E}}^{l} + a_{\mathrm{S}}^{l}I_{\mathrm{S}}^{l} + a_{\mathrm{N}}^{l}I_{\mathrm{N}}^{l} + a_{\mathrm{B}}^{l}I_{\mathrm{B}}^{l} + a_{\mathrm{T}}^{l}I_{\mathrm{T}}^{l} + b^{l} \tag{3}$$

where

$$a_{\mathrm{E}}^{l} = \max\left(A_{\mathrm{w}}D_{\mathrm{cw}}^{l}\left(\frac{1-f}{f}\right) - A_{\mathrm{e}}D_{\mathrm{ce}}^{l}, 0\right)$$
$$a_{\mathrm{w}}^{l} = \max\left(A_{\mathrm{e}}D_{\mathrm{ce}}^{l}\left(\frac{1-f}{f}\right) - A_{\mathrm{w}}D_{\mathrm{cw}}^{l}, 0\right) \tag{4a}$$

$$a_{\mathrm{N}}^{l} = \max\left(A_{\mathrm{s}}D_{\mathrm{cs}}^{l}\left(\frac{1-f}{f}\right) - A_{\mathrm{n}}D_{\mathrm{cn}}^{l}, 0\right)$$
$$a_{\mathrm{S}}^{l} = \max\left(A_{\mathrm{n}}D_{\mathrm{cn}}^{l}\left(\frac{1-f}{f}\right) - A_{\mathrm{s}}D_{\mathrm{cs}}^{l}, 0\right) \tag{4b}$$

$$a_{\mathrm{T}}^{l} = \max\left(A_{\mathrm{b}}D_{\mathrm{cb}}^{l}\left(\frac{1-f}{f}\right) - A_{\mathrm{t}}D_{\mathrm{ct}}^{l}, 0\right)$$
$$a_{\mathrm{B}}^{l} = \max\left(A_{\mathrm{t}}D_{\mathrm{ct}}^{l}\left(\frac{1-f}{f}\right) - A_{\mathrm{b}}D_{\mathrm{cb}}^{l}, 0\right) \tag{4c}$$

$$a_{\mathrm{P}}^{l} = \max\left(\frac{A_{\mathrm{e}}D_{\mathrm{ce}}^{l}}{f}, 0\right) + \max\left(\frac{A_{\mathrm{w}}D_{\mathrm{cw}}^{l}}{f}, 0\right) + \max\left(\frac{A_{\mathrm{n}}D_{\mathrm{cn}}^{l}}{f}, 0\right) + \max\left(\frac{A_{\mathrm{s}}D_{\mathrm{cs}}^{l}}{f}, 0\right) + \beta_{\mathrm{P}}\Delta V_{\mathrm{P}}\Delta\Omega^{l} \tag{4d}$$

$$b^{l} = S_{\mathrm{P}}^{l}\Delta V_{\mathrm{P}}\Delta\Omega^{l} \tag{4e}$$

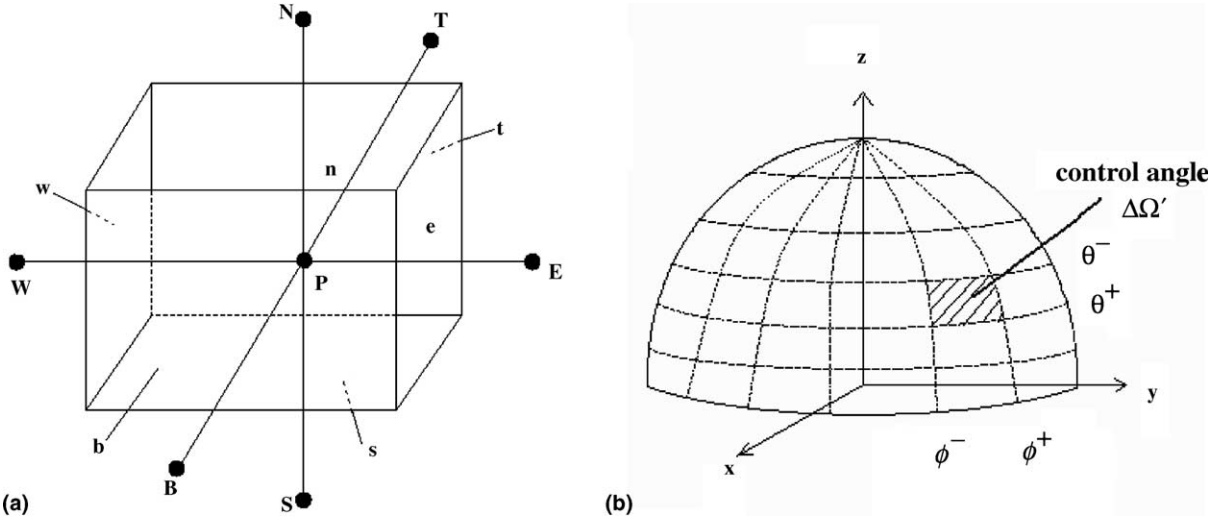

Fig. 1. (a) Schematic of a 3-D control volume, (b) a typical control angle.

$$D^l_{ce} = \int_{\Delta\Omega^l} (\hat{s}^l \cdot \hat{e}_e)\,d\Omega, \quad D^l_{cn} = \int_{\Delta\Omega^l} (\hat{s}^l \cdot \hat{e}_n)\,d\Omega,$$
$$D^l_{ct} = \int_{\Delta\Omega^l} (\hat{s}^l \cdot \hat{e}_t)\,d\Omega, \quad D^l_{cw} = -D^l_{ce},$$
$$D^l_{cs} = -D^l_{cn} \quad \text{and} \quad D^l_{cb} = -D^l_{ct} \tag{5}$$

Here in the above equations, $\hat{e}_e$, $\hat{e}_n$ and $\hat{e}_t$ are the unit area vectors perpendicular to the east, north and top faces, respectively. For Cartesian coordinates, they become x-, y- and z-directions.

In Eqs. (4a)–(4e), A_e, A_w, A_n, A_s, A_t and A_b are the face areas of east, west, north, south, top and bottom faces, respectively and f is the interpolation factor to relate the cell face intensities to the node intensities which value lies between 1 and 0.5. It is termed as a step scheme for $f = 1$ and as a diamond scheme for $f = 0.5$.

The solid angle $\Delta\Omega^l$ in Eq. (4e) is integrated analytically as

$$\Delta\Omega^l = \int_{\phi-\frac{d\phi}{2}}^{\phi+\frac{d\phi}{2}} \int_{\theta-\frac{d\theta}{2}}^{\theta+\frac{d\theta}{2}} \sin\theta\,d\theta\,d\phi$$
$$= d\phi\left[\cos\left(\theta - \frac{d\theta}{2}\right) - \cos\left(\theta + \frac{d\theta}{2}\right)\right] \tag{6}$$

For an isotropically scattering medium, the source term S^l_P in Eq. (4e), can be calculated as

$$S^l_P = \kappa_P I_{b,P} + \frac{\sigma_P}{4\pi} \sum_{l'=1}^{L} I^{l'}_P \Delta\Omega^{l'} \tag{7}$$

where the black body radiation term can be calculated as

$$I_{b,P} = \frac{\sigma_P T^4_P}{\pi} \tag{8}$$

The intensity direction $\hat{s}$ in Eq. (5) is defined as

$$\hat{s} = (\sin\theta\cos\phi)\hat{e}_x + (\sin\theta\sin\phi)\hat{e}_y + (\cos\theta)\hat{e}_z \tag{9}$$

In Eq. (9), θ and ϕ are the polar and azimuthal angle measured as shown in Fig. 2.

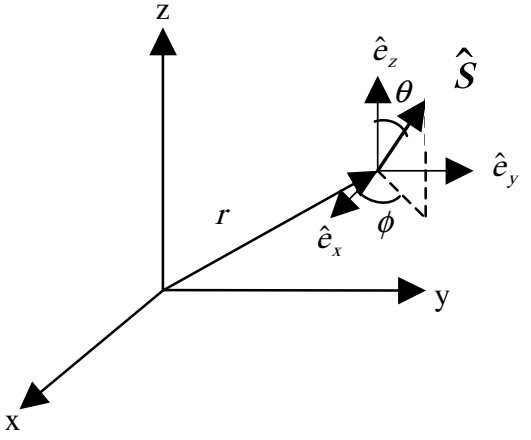

Fig. 2. A typical angular direction.

The calculation of the volume ΔV_P and the area vectors $\hat{e}_e$, $\hat{e}_n$ and $\hat{e}_t$ are according to the formulation of curvilinear coordinates and is not explained here.

2.1. Calculation of incident radiation G

The incident radiation G is calculated as:

$$G(\vec{r}) = \int_{4\pi} I(\vec{r},\hat{s})\,d\Omega = \int_{\phi=0}^{2\pi}\int_{\theta=0}^{\pi} I\sin\theta\,d\theta\,d\phi$$
$$= \sum_{k=1,m} I_k wf_k \tag{10}$$

where $wf_k = d\phi\cos(\theta_k - \frac{d\theta}{2}) - \cos(\theta_k + \frac{d\theta}{2})$.

2.2. Calculation of heat flux q

The heat flux q in x-, y- and z-directions can be calculated as

$$q_x(\vec{r}) = \int_{2\pi} I(\vec{r},\hat{s})(\vec{r}\cdot\hat{e}_x)\,d\Omega$$
$$= \int_{\phi=0}^{2\pi}\int_{\theta=0}^{\pi} I\sin\theta\cos\phi\sin\theta\,d\theta\,d\phi$$
$$= \sum_{k=1,m} I_k wfx_k \tag{11a}$$

$$q_y(\vec{r}) = \int_{2\pi} I(\vec{r},\hat{s})(\vec{r}\cdot\hat{e}_y)\,d\Omega$$
$$= \int_{\phi=0}^{2\pi}\int_{\theta=0}^{\pi} I\sin\theta\sin\phi\sin\theta\,d\theta\,d\phi$$
$$= \sum_{k=1,m} I_k wfy_k \tag{11b}$$

$$q_z(\vec{r}) = \int_{2\pi} I(\vec{r},\hat{s})(\vec{r}\cdot\hat{e}_z)\,d\Omega$$
$$= \int_{\phi=0}^{2\pi}\int_{\theta=0}^{\pi} I\cos\theta\sin\theta\,d\theta\,d\phi$$
$$= \sum_{k=1,m} I_k wfz_k \tag{11c}$$

where the weight factors wfx, wfy, wfz can be integrated analytically between the limits $\theta \pm \frac{d\theta}{2}$ and $\phi \pm \frac{d\phi}{2}$ as

$$wfx = \int (\sin\theta\cos\phi)\sin\theta\,d\theta\,d\phi$$
$$= 0.5\left[\sin\left(\phi + \frac{d\phi}{2}\right) - \sin\left(\phi - \frac{d\phi}{2}\right)\right]$$
$$\times [d\theta - 0.5(\sin\{2\theta + d\theta\} - \sin\{2\theta - d\theta\})] \tag{12a}$$

$$wfy = \int (\sin\theta\sin\phi)\sin\theta\,d\theta\,d\phi$$
$$= 0.5\left[\cos\left(\phi - \frac{d\phi}{2}\right) - \cos\left(\phi + \frac{d\phi}{2}\right)\right]$$
$$\times [d\theta - 0.5(\sin\{2\theta + d\theta\} - \sin\{2\theta - d\theta\})] \tag{12b}$$

$$wfz = \int \cos\theta \sin\theta \, d\theta \, d\phi = \frac{d\phi}{4}(\cos\{2\theta - d\theta\} - \cos\{2\theta + d\theta\}) \quad (12c)$$

2.3. Solution procedure

The discretization results in a set of algebraic equation of intensity. The marching procedure adopted here is similar to Chai et al. [4] and hence is not discussed here. Due to 3-D nature, we have eight marching directions as compared to four marching directions in case of the 2-D problems of Chai and Moder [7].

2.4. Multiblocking strategy

The transformation of information between neighbouring blocks is done with the help of overlapping blocks.

A typical 2-D block arrangement is shown in Fig. 3. The two blocks are extended towards each other to exchange a particular variable as shown in Fig. 3. The information from block 1 is carried via the nodes 21–25 to the block 2 by the nodes 31–35. That means any variable (var) of interests at the overlapping nodes of block 1 to block 2 are copied as: var(31) = var(21), var(32) = var(22) and so on. Similarly the block 1 copies the information from block 2 as: var(26) = var(36), var(27) = var(37) and so on. The procedure gives complete conservation of radiant energy between the blocks.

3. Results and discussion

Several problems are solved to check the validity of the present work. First, the 3-D code is validated with the results available in the literature. A unit cubical enclosure with one block is considered for this purpose. The same geometry is then divided into four blocks and the results are compared with the one block results to validate the multiblocking procedure. In the next problem, an L-shaped geometry is considered whose results

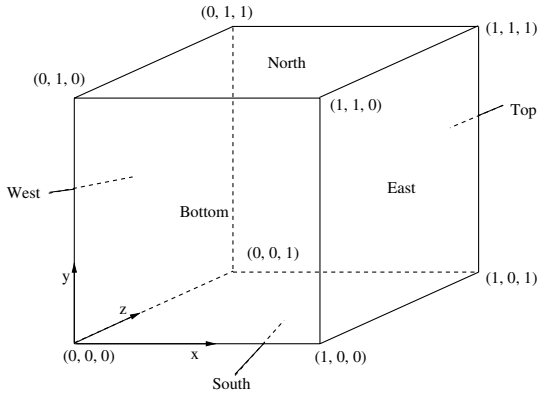

Fig. 4. Unit cube under consideration.

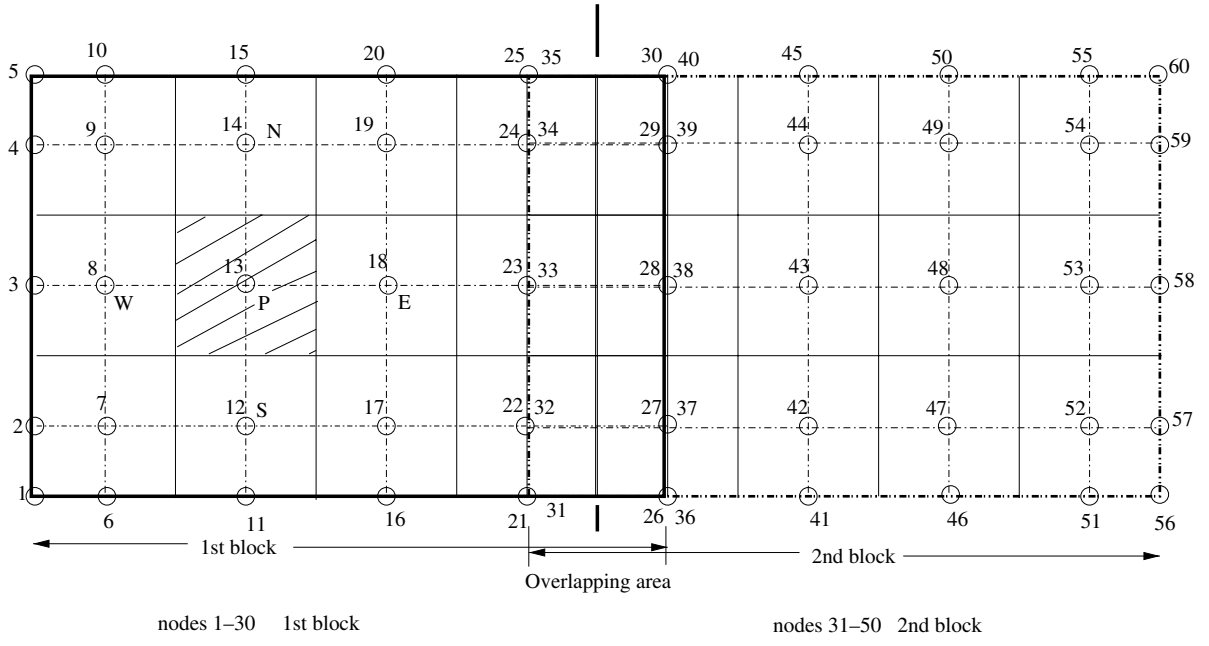

Fig. 3. Blocking strategy.

are compared with results available in the literature. A complex geometry with 16 blocks are considered to show the applicability of the present work in the fourth problem. In the last problem, a J-shaped enclosure is considered to show the applicability of the present blocking procedure for inclined planes. Problems are considered with both the radiative equilibrium and non-radiative equilibrium situations. The medium is assumed to be participating with different optical properties.

3.1. Problem 1

A unit cubical enclosure is considered (Fig. 4) as discussed by Fiveland [17]. The walls of the enclosures are considered to be radiatively black ($\varepsilon = 1$) and a radiative equilibrium situation is considered. Three boundaries are at unit emissive power ($= \varepsilon\sigma T_h^4 = 1$, T_h is the temperature of these boundaries) viz. east boundary ($x = 1$), south boundary ($y = 0$) and bottom boundary ($z = 0$). The other boundaries are cold with zero emissive power.

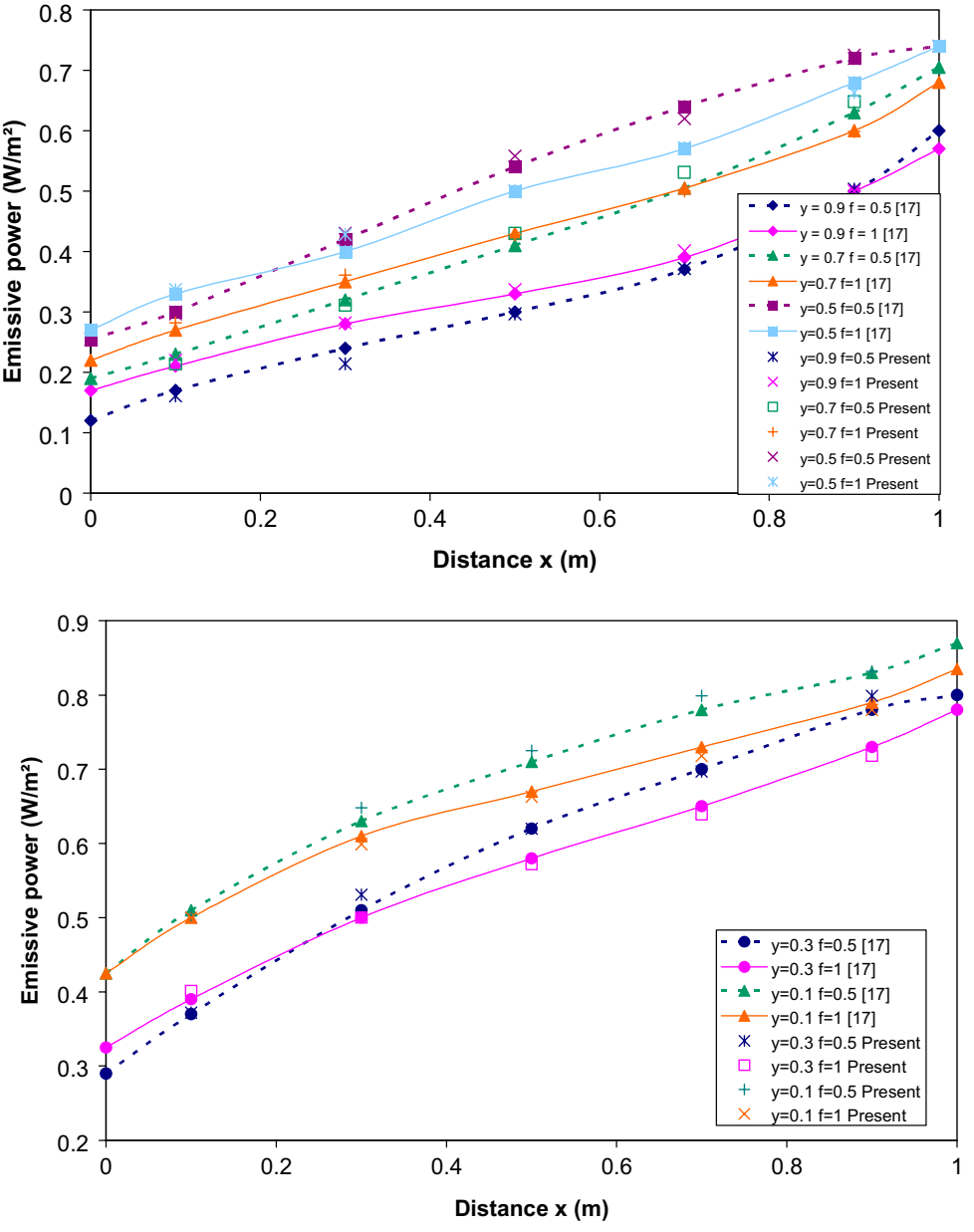

Fig. 5. Comparison of results of a 3D geometry having one block with literature.

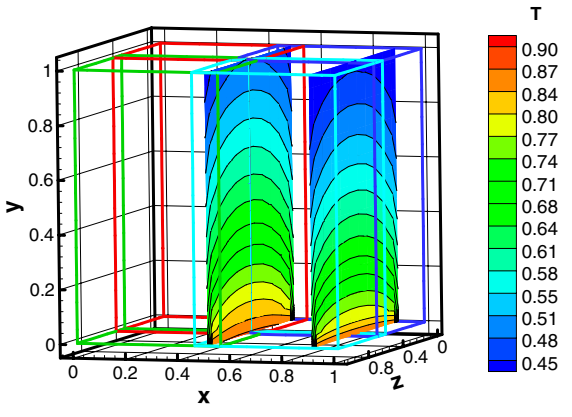

Fig. 6. Isotherms for a geometry with 4 blocks.

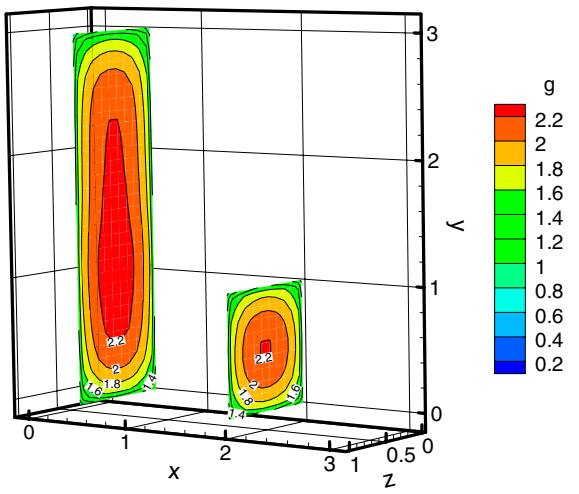

Fig. 8. Contours of incident radiation distribution g at $x = 0.5$ and $x = 2.0$.

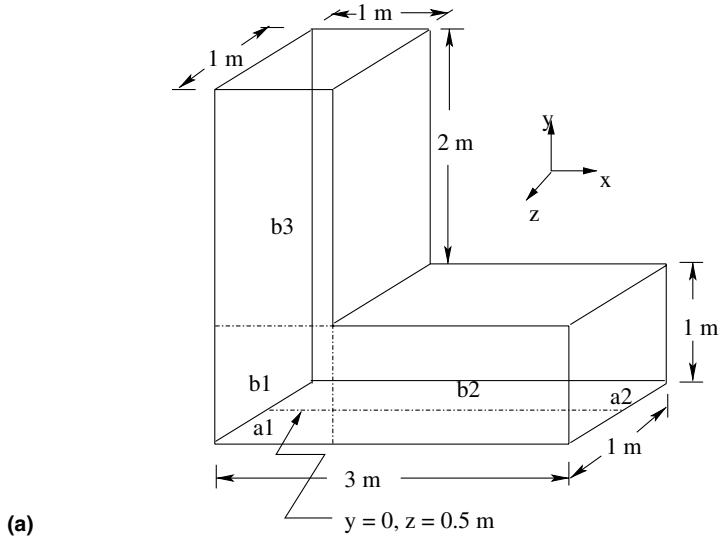

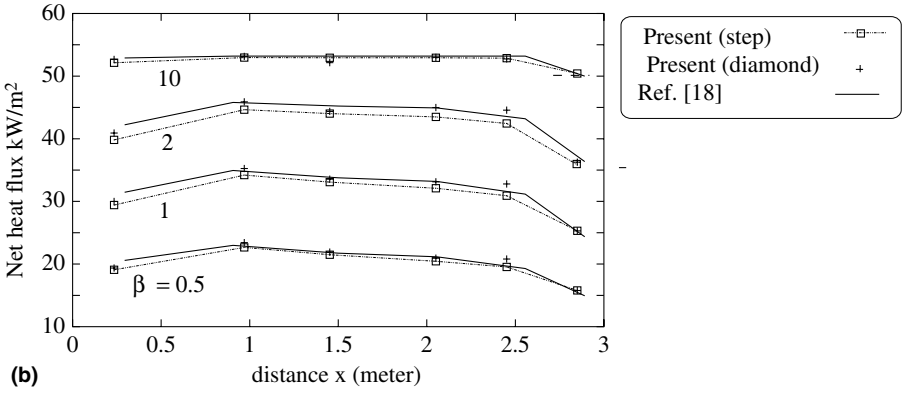

Fig. 7. (a) L-shaped enclosure under consideration. (b) Comparison of heat flux distributions with the literature.

The medium has an extinction coefficient of $\beta = 1.0$. The results of emissive power ($=\sigma T^4$) are shown in Fig. 5. The results are shown at a plane $z = 0.5$ and along different lines at $y = 0.1$, 0.3, 0.5, 0.7 and 0.9. The number of control volumes and control angles considered are $10 \times 10 \times 10$ and 10×8 ($\theta \times \phi$), respectively and both step and diamond scheme are considered for comparison of the results. It is seen that the results compare well with the discrete ordinates results of Fiveland [17].

3.2. Problem 2

Having validated the code with one block in the first problem, the accuracy of the multiblocking procedure is discussed here in this problem with a radiative equilibrium situation. Same unit enclosure is considered. The south boundary ($y = 0$) is assumed to be hot ($T = 1$) while other boundaries are assumed to be cold ($T = 0$). All boundaries are black and the medium is isotropically scattering with an extinction coefficient $\beta = 1.0$.

The whole 3-D domain is divided into four blocks as shown in Fig. 6. The results with four blocks are compared with the results taking the whole domain as a single block. Results are found to be exactly the same. Temperature contours are shown in Fig. 6 at two different locations. Since results are exactly the same for multiblocking and single blocking, only one set of plots are visible. The number of control volumes and control angles considered are $10 \times 10 \times 10$ and 10×8 ($\theta \times \phi$), respectively and the step scheme is considered for interpolation. The accuracy of the results is not the issue of the current problem and so only a reasonable number of control volumes and control angles are considered and no further attempt is tried to optimize the results with spatial and angular grids.

3.3. Problem 3

The third problem considered is an L-shaped enclosure previously considered by Malalasekera and James [18]. They used a body fitted grid with the discrete trans-

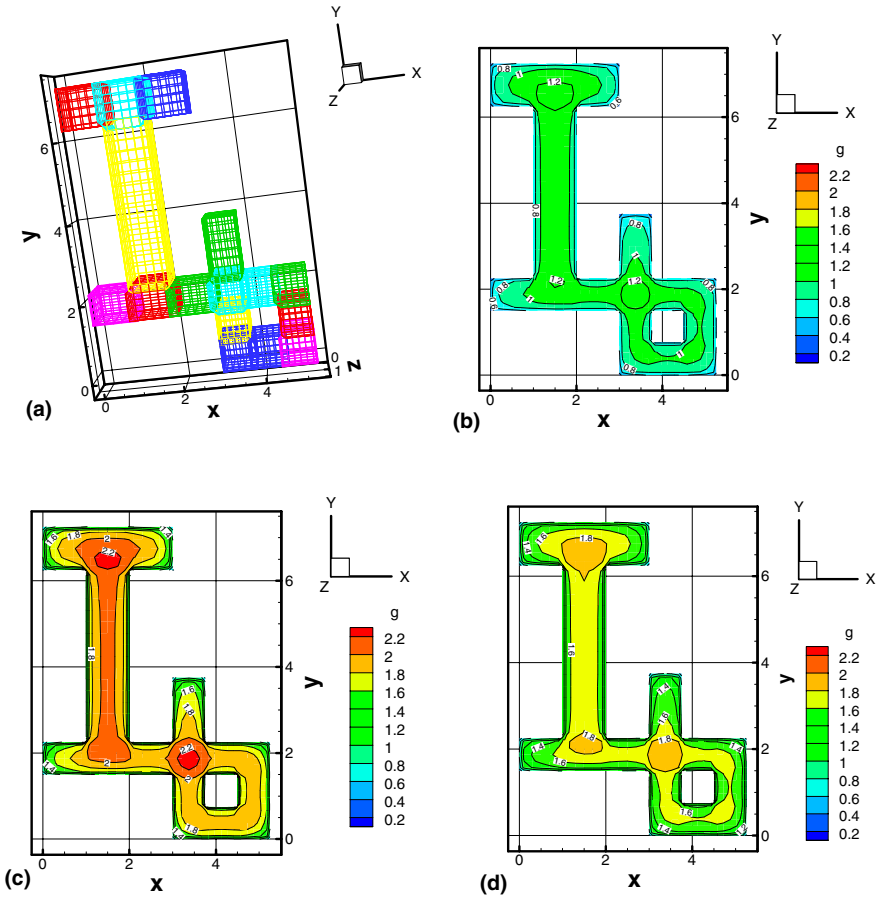

Fig. 9. (a) Geometry and mesh of the I_b shaped enclosure, (b) contours of incident radiation g at $z = 0.5$ and $\omega = 0.5$, (c) contours of g at $z = 0.5$ and $\omega = 0$, (d) contours of g at $z = 0.1$ and $\omega = 0$.

fer method used to solve the RTE. An absorbing, emitting medium is considered with an uniform temperature of 1000 K. The boundaries are black and at 500 K. Different extinction coefficients viz. $\beta = 0.5$, 1.0, 2.0 and 10.0 are considered. The net heat flux along the line $a1a2$ (Fig. 7(a)) is shown in Fig. 7(b) for different extinction coefficients. Both step and diamond schemes are used and results are found to be similar with the results of [18]. The L-shaped enclosure is divided into three blocks and a total of $50 \times 30 \times 10$ numbers of control volume with a 10×8 ($\theta \times \phi$) control angles are considered for sufficient agreement with [18]. It is to be noted here that the grid quality in the present case is better than the body fitted grids of [18]. The contour of incident radiation $g(= \frac{G}{\sigma T_{\text{ref}}^4},\ T_{\text{ref}} = 1000)$ is shown in Fig. 8 with two different slices at $x = 0.5$ and $x = 2.0$. The results show correct physical trend of the present problem.

3.4. Problem 4

The fourth problem considered is a similar problem considered by Chai et al. for a 2-D geometry with multiblocking [7]. The similar geometry is extended here in the third dimension. The enclosure looks like the letter I_b. All boundaries are considered to be cold ($T = 0$) and black and the medium is at some uniform temperature T_m. An extinction coefficient $\beta = 1$ is considered.

A total of 16 blocks are considered for this problem. In Fig. 9(a), the mesh and the blocks considered in this works are shown. The step scheme is considered here and a control angle of 10×8 ($\theta \times \phi$) is considered for angular discretization.

In Fig. 9(b)–(d), contour plots for incident radiation $g(= \frac{G}{\sigma T_{\text{ref}}^4},\ T_{\text{ref}} = T_m)$ are shown at different position and different conditions. In Fig. 9(b), g distributions are shown for the scattering albedo $\omega = 0.5$. The position of the slice is at $z = 0.5$. This can be compared with Fig. 9(b) which is also drawn at the same position with a scattering albedo $\omega = 0$. With higher scattering, the medium losses more heat to the surroundings and results in a lower value of g which can be seen from Fig. 9(b). The average g distribution range is lower in this case than in Fig. 9(c). Fig. 9(d) shows the g distribution at the location $x = 0.1$ with the other conditions same as in Fig. 9(c). It is seen that the value of g decreases as soon as the slice moves towards the boundary. The trends observed from these plots are physically correct and also similar to the plots shown by Chai and Moder [7] for their 2-D geometry.

3.5. Problem 5

In Fig. 10(a) and (b), a J-shaped enclosure is considered to show the applicability of the work to a body-fitted curvilinear grid. The geometry is similar to the 2-D geometry previously considered by Chai et al. [5]. The same geometry is extended in z-direction by 0.4 m. The geometry can be understood from Fig. 10(a). The mesh consists of three blocks and a mesh size of total $11 \times 30 \times 6$ is used in x-, y- and z-directions. A control angle of 10×8 ($\theta \times \phi$) is considered with step scheme

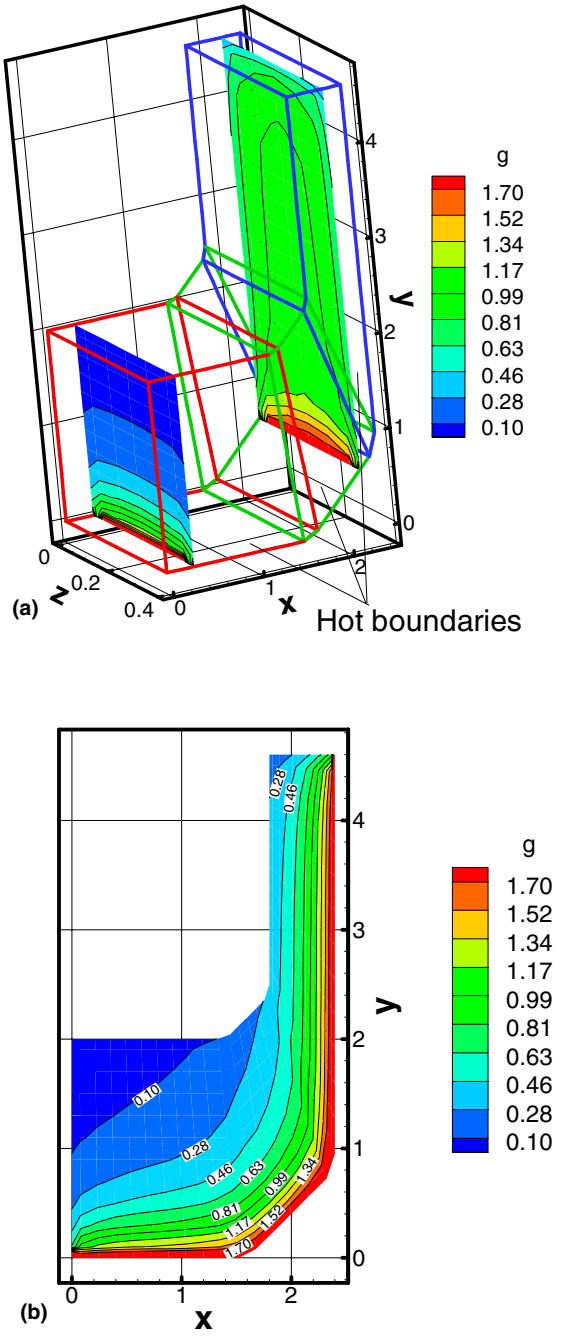

Fig. 10. Contours of incident radiation g of a J-shaped enclosure at slices (a) $x = 0.3$ and 2.2, (b) $z = 0.2$.

used for interpolation. The south boundaries are hot and at temperature T_h and others are assumed as cold as shown in Fig. 10(a). In Fig. 10(a), contours of incident radiation $g(=\frac{G}{\sigma T_{ref}^4},\ T_{ref}=T_h)$ are shown at two different locations $x=0.3$ and $x=2.2$. Since the slice at $x=2.2$ is closer to the hot boundary, higher g distributions can be observed in comparison to the slice at $x=0.3$. The contour plot of g is shown at position $z=0.2$ in Fig. 10(b). All the plots are similar to the plots of Chai et al. [5] for 2-D calculations. In both the figures, plots show the correct trend with the imposed boundary conditions.

4. Summary

The finite volume method is applied for 3-D curvilinear coordinates with a multiblock procedure. Complicated geometries can be simulated by dividing the whole domain with several hexahedral blocks. Several problems are solved to show the accuracy and applicability of the proposed multiblocking. Results are found to be promising as they are validated with the existing results of the literature. The proposed procedure has the flexibility to couple with the CFD codes since it is based on the same block-structured grid philosophy as the CFD codes do.

References

[1] G.D. Raithby, E.H. Chui, A finite volume method for predicting radiant heat transfer in enclosures with participating media, J. Heat Transfer 112 (1990) 415–423.
[2] E.H. Chui, G.D. Raithby, P.M.J. Hughes, Prediction of radiative transfer in cylindrical enclosures by the finite volume method, J. Thermophys. Heat Transfer 6 (4) (1992) 605–611.
[3] E.H. Chui, G.D. Raithby, Computation of radiant heat transfer on a nonorthogonal mesh using the finite volume method, Numer. Heat Transfer 23 (1993) 269–288.
[4] J.C. Chai, H.S. Lee, S.V. Patankar, Finite volume method for radiation heat transfer, J. Thermophys. Heat Transfer 8 (3) (1994) 419–425.
[5] J.C. Chai, H.S. Lee, S.V. Patankar, Treatment of irregular geometries using a Cartesian coordinates finite-volume radiation heat transfer procedure, Numer. Heat Transfer, Part B 26 (1994) 225–235.
[6] J.C. Chai, G. Parthasarathy, H.S. Lee, S.V. Patankar, Finite volume radiation heat transfer procedure for irregular geometries, J. Thermophys. Heat Transfer 9 (3) (1995) 410–415.
[7] J.C. Chai, J.P. Moder, Spatial-multiblock procedure for radiation heat transfer, Numer. Heat Transfer, Part B 31 (1997) 277–293.
[8] K.C. Karki, S.V. Patankar, Calculation procedure for viscous incompressible flows in complex geometries, Numer. Heat Transfer 14 (1988) 295–307.
[9] K.C. Karki, S.V. Patankar, Solution of some two-dimensional incompressible flow problems using a curvilinear coordinate system based calculation procedure, Numer. Heat Transfer 14 (1998) 309–321.
[10] K.C. Karki, S.V. Patankar, Pressure based calculation procedure for viscous flows at all speeds in arbitrary configurations, AIAA J. 27 (9) (1989) 1167–1174.
[11] I. Demirdzic, A.D. Gosman, R.I. Issa, A finite volume method for the prediction of turbulent flow in arbitrary geometries, in: International Conference on Numerical Methods in Fluid Dynamics, 7th, Stanford and Moffett Field, CA, June 23–27, 1980, Proceedings (A82-24426 10-02), Springer-Verlag, Berlin and New York, 1981, pp. 144–150.
[12] M. Peric, A Finite Volume Method for the Prediction of Three Dimensional Fluid Flow in Complex Duct, Ph.D. Thesis, University of London, London, 1985.
[13] W. Shyy, S.S. Tong, S.M. Correa, Numerical recirculating flow calculations using a body-fitted coordinate system, Numer. Heat Transfer 8 (1985) 99–113.
[14] C.M. Rhie, W.L. Show, Numerical study of the turbulent flow past and airfoil with trailing edge separation, AIAA J. 21 (1983) 1525–1532.
[15] J.Y. Murthy, S.R. Mathur, A finite volume method for radiative heat transfer using unstructured meshes, AIAA-98-0860, January 1998.
[16] J.Y. Murthy, S.R. Mathur, Radiative heat transfer in axisymmetric geometries using an unstructured finite-volume method, Numer. Heat Transfer, Part B 33 (1998) 397–416.
[17] W.A. Fiveland, Three-dimensional radiative heat-transfer solutions by the discrete-ordinate method, J. Thermophys. Heat Transfer 2 (4) (1988) 309–316.
[18] W.M.G. Malalasekera, E.H. James, Radiative heat transfer calculations in three-dimensional complex geometries, J. Heat Transfer 118 (1996) 225–228.